Journal of Controlled Release 294 (2019) 247–258

Contents lists available at ScienceDirect

Journal of Controlled Release

journal homepage: www.elsevier.com/locate/jconrel

Fibrin-hyaluronic acid hydrogel-based delivery of antisense oligonucleotides for ADAMTS5 inhibition in co-delivered and resident joint cells in osteoarthritis

João Pedro Garcia[a], Jeroen Stein[a], Yunpeng Cai[b], Frank Riemers[c], Ezequiel Wexselblatt[d], Jesper Wengel[e], Marianna Tryfonidou[c], Avner Yayon[d], Kenneth A. Howard[b], Laura B. Creemers[a,*]

[a] Department of Orthopedics, University Medical Center Utrecht, the Netherlands
[b] Interdisciplinary Nanoscience Center (iNANO), Department of Molecular Biology and Genetics, Aarhus University, Denmark
[c] Department of Clinical Sciences of Companion Animals, Faculty of Veterinary Medicine, Utrecht University, the Netherlands
[d] ProCore Biomed Ltd, Israel
[e] Nucleic Acid Center, University of Southern Denmark, Denmark

ARTICLE INFO

Keywords:
Antisense oligonucleotide
Gapmer
Hydrogel
Osteoarthritis
ADAMTS5
Chondrocytes

ABSTRACT

To date no disease-modifying drugs for osteoarthritis (OA) are available, with treatment limited to the use of pain killers and prosthetic replacement. The ADAMTS (A Disintegrin and Metallo Proteinase with Thrombospondin Motifs) enzyme family is thought to be instrumental in the loss of proteoglycans during cartilage degeneration in OA, and their inhibition was shown to reverse osteoarthritic cartilage degeneration. Locked Nucleic Acid (LNA)-modified antisense oligonucleotides (gapmers) released from biomaterial scaffolds for specific and prolonged ADAMTS inhibition in co-delivered and resident chondrocytes, is an attractive therapeutic strategy. Here, a gapmer sequence identified from a gapmer screen showed 90% *ADAMTS5* silencing in a monolayer culture of human OA chondrocytes. Incorporation of the gapmer in a fibrin-hyaluronic acid hydrogel exhibited a sustained release profile up to 14 days. Gapmers loaded in hydrogels were able to transfect both co-embedded chondrocytes and chondrocytes in a neighboring gapmer-free hydrogel, as demonstrated by flow cytometry and confocal microscopy. Efficient knockdown of *ADAMTS5* was shown up to 14 days in both cell populations, *i.e.* the gapmer-loaded and gapmer-free hydrogel. This work demonstrates the use applicability of a hydrogel as a platform for combined local delivery of chondrocytes and an ADAMTS-targeting gapmer for catabolic gene modulation in OA.

1. Introduction

Osteoarthritis (OA) is the most common joint disorder in the aged population, and a leading cause of morbidity worldwide due to functional impairment and pain [1]. Defined as a chronic and progressive disease of the whole joint, OA is predominantly characterized by cartilage degeneration, subchondral sclerosis, osteophyte formation, and inflammation of the synovial capsule [1,2]. At the cellular level, OA is marked by an increased production of catabolic molecules leading to progressive and irreversible loss of collagen and aggrecan [1,3]. To date, disease modifying therapies remain unavailable, and OA treatment is limited to corticosteroid administration for pain relief and prosthetic replacement of the affected joints at an end stage [1,4,5]. One feature correlated with pain and radiographic stage in OA patients is the presence of cartilage lesions of variable size [6–8]. These are generally a result of weakening of the joint and a factor highly associated with disease progression [9]. Such lesions may be a viable target for regenerative approaches. Autologous chondrocyte implantation (ACI), or MACI (matrix-assisted ACI) have shown to be effective in repair of focal lesion of the cartilage after joint trauma, but such approach will not be viable in the OA joint, as long as both the transplanted cells and those in the neighboring tissue are in a permanently catabolic state [10].

Among the major catabolic factors in OA, the matrix degrading ADAMTS (a disintegrin and metallo proteinase with thrombospondin motifs) family, in particular ADAMTS4 and ADAMTS5, were shown to be instrumental in the degenerative events that lead to OA [11,12]. These enzymes are known to be synthetized not only by chondrocytes but also other joint tissues, such as the synovium [13]. Inhibition of these proteases prevented degradation both in human cartilage explants

* Corresponding author.
E-mail address: l.b.creemers@umcutrecht.nl (L.B. Creemers).

https://doi.org/10.1016/j.jconrel.2018.12.030
Received 10 December 2018; Accepted 16 December 2018
Available online 18 December 2018
0168-3659/ © 2019 Published by Elsevier B.V.

[12,14,15] and in animal models of OA, even reversing cartilage degeneration [16–18]. Hence, their inhibition is a promising therapeutic approach in OA. Nevertheless, non-specific small molecule drugs can cause side effects upon systemic administration and are, even if administered locally, rapidly cleared resulting in reduced duration of action [19].

Gene silencing strategies have shown great potential in overcoming these setbacks [20]. However, the efficiency of small interfering RNAs is dependent on viral or non-viral vectors for cellular internalization, which can pose additional issues regarding toxicity [20,21]. In this regard, locked nucleic acid (LNA)-modified gapmers are a particularly attractive alternative. Gapmers are single stranded antisense oligonucleotides (ASOs) composed by a central block of DNA flanked by modified nucleotides [22]. Once inside the cell, gapmers arrest protein translation by activation of RNAse H1-mediated messenger RNA (mRNA) cleavage or steric hindrance of the splicing or translational machinery [23]. The presence of LNAs together with phosphorothioate (PS) backbone modifications confer improved stability and resistance to endonuclease degradation, hence improving the pharmacokinetic profiles [22,24]. Together with the smaller size of the molecule, these modifications are thought to promote unassisted cellular internalization by a process denominated "gymnosis" [25–29].

Even though chemical modifications of ASOs have been shown to enhance silencing potency and pharmacokinetic profiles with concomitant prolongation of effects [23], rapid systemic clearance may still reduce longevity of therapeutic efficacy. Additionally, intravenous administration might further limit drug bioavailability in avascular tissues such as cartilage. Hence, direct intra-articular administration in controlled release systems can minimize systemic side-effects while allowing for a higher and prolonged bioavailability of the therapeutics in the joint environment [19,30]. Biomaterial carriers, such as hydrogels, are ideally suited as local sustained release reservoir for drugs [19,30–32].

We hypothesize that the combination of chondrocytes and ASOs in a hydrogel scaffold for resurfacing and treatment of focal lesions in OA joints will provide prolonged inhibition of ADAMTS expression both in transplanted chondrocytes and surrounding joint tissue cells. Ultimately, this treatment strategy targets OA by sustained silencing of OA-related genes in combination with cell therapy for regeneration. Here, we show proof of principle for this approach by using a fibrin (F) and hyaluronic acid (HA) hydrogel (F:HA) as a platform for combined delivery of cells and an ADAMTS5-targeting ASO in a novel *in vitro* system mimicking chondrocyte delivery for cartilage resurfacing and its interaction with surrounding native joint tissues exposed to a pro-inflammatory environment.

2. Materials and methods

2.1. Materials

The F:HA hydrogel at a ratio of 3.2:1 was manufactured and provided by ProCore Bio-med Inc. (Israel), at final concentrations of 6.21 and 1.94 mg/ml of fibrinogen and HA, respectively. ASOs sequences were designed by JW and YC and purchased from Eurogentec (Netherlands).

All ASOs were synthesized as all-phosphorothioate linked sequences except for the Cy5-labeled gapmer, which was synthesized as an all-phosphorodiester sequence (Table 1). The golden standard siRNA was used as a control. Previously described siRNA sequences targeting *ADAMTS5* and β-catenin interacting protein 1 (*CTNNBIP1*) were purchased from Eurogentec (Table 1) [12,33]. *CTNNBIP1* was shown to be a potential off-target of ASO3.

2.2. Cell isolation and culture

Human articular chondrocytes were isolated from articular cartilage from patients with OA undergoing total knee arthroplasty. The anonymous use of redundant tissue for research purposes is part of the standard treatment agreement with patients in the University Medical Center Utrecht and was carried out under protocol n° 15–092 of the UMCU's Review Board of the BioBank. Chondrocytes were isolated by mincing and subsequently digesting the cartilage overnight at 37 °C in Dulbecco's Modified Eagle's Medium Glutamax (DMEM, Thermo Fischer Scientific) supplemented with 0.15% (*w/v*) type II collagenase (Worthington Biochemical Corporation), 10% (*v/v*) Fetal Bovine Serum (FBS, Biowest) and 100 U/ml penicillin and streptomycin (Gibco).

Undigested debris were removed using a 70 μm cell strainer followed by a PBS wash. Cells were subsequently plated and grown in a humidified incubator at 37 °C with expansion medium consisting of DMEM supplemented with 10% FBS, 0.2 nM ascorbic-2-phosphate (Sigma-Aldrich), 100 U/ml penicillin and streptomycin and 10 ng/ml basic fibroblast growth factor (bFGF, R&D Systems). Medium was renewed every 3 days. Cells were expanded until passage one and either frozen or further expanded and used for experiments at passage 2.

2.3. Gene knockdown in monolayer

The four different ASO were tested in order to choose the most potent one resulting in sufficient silencing of ADAMTS5. Human articular chondrocytes were plated at a density of 1×10^5 cells per well in 24-well plates and grown in DMEM containing 100 U/ml of penicillin and streptomycin, 0.2 nM Ascorbic-2-Phosphate, 1 × Insulin-Transferrin-Selenium-Ethanolamine (ITS-X, Thermo Fischer Scientific) and 50 μg/ml L-proline (Sigma-Aldrich) for 24 h in a humidified incubator at 37 °C and 5% CO_2. Gapmers were diluted in medium and added to the cells at a final concentration of 1 μM. Cells were cultured for an additional 72 h and expression levels of *ADAMTS5* were determined by Real-Time PCR (qPCR). Fold change in gene expression was evaluated compared to non-treated cells as described in section 2.10. For screening experiments, the housekeeping gene *18S* was used for normalization of *ADAMTS5* expression.

Cytotoxicity of the gapmers was determined by measuring cellular lactate dehydrogenase (LDH) release using the Cytotoxicity Detection KitPLUS (Roche) according to the manufacturer's instructions. Culture media were collected 24 h after adding the ASOs to the cells. The LDH activity in culture supernatant was measured at 490 nm and 680 nm with a Benchmark Microplate reader (Bio-Rad). Viability of cells transfected with ASOs was calculated according to the manufacturer's instructions.

A similar experiment was set up to evaluate the effect of siRNA-mediated *CTNNBIP1* silencing on *ADAMTS5* expression. Cells were cultured as described above, transfected with anti-CTNNBIP1 siRNA (20 nM) and Lipofectamine RNAiMAX (Thermo Fischer Scientific) and further cultured for 72 h. Gene expression analysis of *ADAMTS5* and *CTNNBIP1* was performed as described above.

2.4. Dose response of gapmer-mediated ADAMTS5 silencing in TNF-α/OSM-stimulated OA chondrocytes

Human articular chondrocytes were plated at a density of 1×10^5 cells per well in 24-well plates and grown in DMEM medium containing 100 U/ml of penicillin and streptomycin, 0.2 nM ascorbic-2-phosphate, 50 ng/ml L-proline in a humidified incubator at 37 °C, 5% CO_2. After 24 h tumor necrosis factor alpha (TNF-α) and oncostatin M (OSM) were added to the cells at concentrations of 10 and 1 ng/ml, respectively, to provide pro-inflammatory stimuli and thereby mimic a catabolic environment and enhancing *ADAMTS5* expression.

Gapmer 3 was added to the cells at concentrations of 100, 250, 500 and 1000 nM. As a positive control, anti-ADAMTS5 siRNA (20 nM) was added to the cells using Lipofectamine RNAiMAX according to the manufacturer's instructions. The non-targeting sequence ASO 1 was added at a concentration of 1000 nM as a negative control. Cells were

Table 1
ASOs and siRNA sequences.

ASO ID	Nucleotide sequence	Length
ASO 1 (non-targeting)	5′- lT*lA*lG*dC*dC*dT*dG*dT*dC*dA*dC*dT*dT*lC*lT*lC 3′	16
ASO 2	5′-lA*lC*lT*lT*dT*dT*dA*dT*dG*dT*dG*dG*dG*lT*lT*lG*lC 3′	17
ASO 3	5′-lC*lT*lT*dT*dT*dA*dT*dG*dT*dG*dG*dG*lT*lT*lG 3′	15
ASO 4	5′-lG*lA*lG*dA*dG*dA*dA*dA*dG*dT*dA*dG*aT*aT*lG 3′	15
Cy5-ASO	5′- Cy5-lClTlTdTdTdAdTdGdTdGdGdGlTlTlG 3′	15
Anti-ADAMTS5 siRNA	Sense strand 5′ -AAGAUAAGCGCUUAAUGUCUU 3′ Anti-sense strand 5′ -AAGACAUUAAGCGCUUAUCUU 3′	21
Anti-CTNNBIP1 siRNA	Sense strand 5′ -GAUGGGAUCAAACCUGACA 3′ Anti-sense strand 5′ -UGUCAGGUUUGAUCCCAUC 3′	19

"l" denotes for locked nucleotide bases. "*" denotes for phosphorothioated DNA bases. "d" denotes for DNA nucleotides.

cultured for an additional 72 h and expression levels of *ADAMTS5* and *18S* (housekeeping gene) were determined by Real-Time PCR (qPCR). Fold change in gene expression was evaluated relatively to non-treated cells.

2.5. Release profiles

To investigate the loading efficiency of the F:HA hydrogel and assess the gapmer-release profiles, Cy5-labeled gapmer was incorporated in 150 and 300 µl of F:HA hydrogel at concentrations of 1 and 5 µM. After mixing the hydrogel and gapmer solutions, 10 µl of human thrombin (50 U/ml) in 1 M $CaCl_2$ were added, followed by a 40-minute incubation at 37 °C in a 5% CO_2 humidified incubator to allow polymerization. Hydrogels were then washed with DMEM medium and fluorescence was measured using Fluoroskan Ascent FL fluorometer (Thermo Fischer Scientific) with an emission/excitation pair of 620/670 nm. DMEM medium was used as release buffer. After t0, hydrogels were incubated in 1 ml release buffer at 37 °C in 5% CO_2 humidified incubator. At every timepoint, release buffer was completely removed, and new buffer added. Fluorescence in the medium was measured immediately after collection at the different timepoints up to 14 days. Loading efficiency of the gapmer on the hydrogels was calculated based on the initial amount of gapmer mixed in the hydrogel minus the non-incorporated gapmer removed during washing. The incorporated amount was then considered as 100% for the subsequent release measurements.

Release was calculated based on a standard curve (10 nM to 1000 nM) of Cy5-gapmer prepared at t0. The series of samples composing the standard curve were incubated together with the hydrogels for the whole experiment, and samples were taken at every timepoint to account for decrease of fluorescence of the Cy5 label over time.

One hydrogel was harvested at day 3 and processed for analysis of gapmer distribution. The hydrogel was fixed in 4% formalin for 10 min followed by 5% PBS-BSA blocking for 30 min. Subsequently, the hydrogel was incubated for 1 h at room temperature with 2 µg/ml anti-fibrinogen antibody (DAKO). Then, Alexa Fluor® 488-labeled secondary antibody rabbit anti-goat (Thermo Fischer) was added at a concentration of 8 µg/ml and incubated for 1 h at room temperature. Between each step, the samples were washed three times with PBS containing 0.05% Tween. Samples were imaged with a Leica SP8X (Leica) confocal microscope. Image processing and analysis was performed using Fiji (National Institutes of Health, Bethesda, USA) software version 1.50 [34].

2.6. Gapmer delivery in hydrogel culture

A 3D *in vitro* model composed of two separate hydrogel constructs was established (Fig. 1): the top hydrogel containing OA chondrocytes (mimicking therapeutically "delivered cells") and gapmers, and the bottom hydrogel containing OA chondrocytes only to represent "resident cells". The top hydrogel was prepared by mixing 150 µl of F:HA hydrogel, 10 µl of cell suspension (2.5×10^5 cells) and 7.5 µl of ASO solution (final concentration 0.1 to 5 µM) in a 2 ml Eppendorf tube, whereas the bottom hydrogel was prepared by mixing the same hydrogel volume with 10 µl of cell suspension (2.5×10^5 cells) in a 48-well plate. For polymerization, thrombin (50 U/ml) was added to the hydrogels followed by incubation at 37 °C for 30 min. After polymerization the top hydrogel was transferred to the 48-well plate upon addition of 1 ml of culture medium. This set-up was used for subsequent experiments.

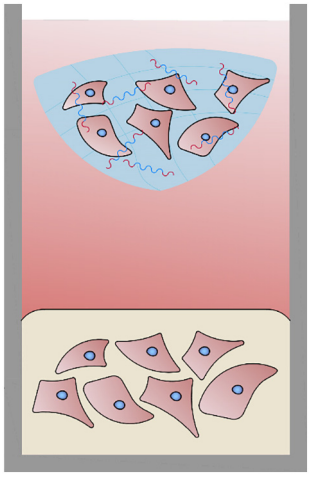


Fig. 1. Scheme of two-hydrogel *in vitro* model. Top hydrogel containing ASOs and OA chondrocytes (mimicking therapeutically "delivered cells"). Bottom hydrogel containing OA chondrocytes only ("resident cells").

2.7. Diffusion and transfection studies

For quantitative assessment of gapmer-cell association, the *in vitro* model described above was cultured for 3 days with 0.1 and 1 µM Cy5-labeled gapmer in the top hydrogel. Upon harvesting the hydrogels were digested separately and processed for flow cytometry analysis. Digestion was carried out at 37 °C for 20 min using 0.25% (*w/v*) trypsin (25,200,056, Thermo Fischer Scientific), followed by filtration through 0.22 µm filters (Merck) to remove hydrogel debris. The cell suspension was centrifuged and resuspended (2×) in ice-cold PBS and stained with 100 ng/ml DAPI for 5 min, staining debris, and apoptotic and dead cells as an additional parameter for population gating. DAPI excess was removed by washing the cells in ice-cold PBS. Finally, cells were resuspended in a flow cytometry buffer (2% BSA, 2 mM EDTA, and 25 mM HEPES) and analyzed using a FACSCanto II (BD Biosciences) flow cytometer for DAPI (FL1 channel: 405 nm excitation laser, 450/40 BP filter) and Cy5 (FL2 channel: 633 nm excitation laser; 620/20 BP filter). Cell doublets and debris were gated out based on forward (FSC) and side (SSC) scatters. DAPI-negative cells were then analyzed for their Cy5 intensity. Ten thousand events were acquired, and data were further analyzed using FlowJo (TreeStar) software version 10.0.

Experiment was performed in triplicate ($n = 3$).

Furthermore, confocal microscopy was performed to assess gapmer diffusion to the bottom hydrogel and transfection of embedded cells. The experimental set up was the same as described above. At the endpoint the hydrogels were washed twice with PBS and fixed in formalin for 1 h, followed by DAPI stain (100 ng/ml) for 1 h to ensure full thickness staining. Samples were imaged axially with a Leica SP8X (Leica) confocal microscope and a 20× objective. Image processing and analysis was performed using Fiji (National Institutes of Health, Bethesda, USA) software version 1.50 [34].

2.8. Subcellular localization of gapmers

To assess subcellular localization of the gapmers, the *in vitro* model was used with a gapmer concentration of 1 μM in the top hydrogel and cultured for 3 days. At the endpoint, digestion of the hydrogels was carried out at 37 °C for 20 min using trypsin, as described previously. Subsequently, the cells were plated in Cellview™ dishes (Greiner Bio-one) and cultured for 24 h to allow cell attachment.

Cells were fixed in 4% formalin for 10 min, followed by permeabilization with 0.2% PBS-Triton for 20 min. Blocking was performed using 5% PBS-BSA for 30 min followed by 1 h incubation at room temperature with 1.25 μg/ml anti-EEA1 (610,456, BD Biosciences) or 1.5 μg/ml anti-LAMP1 (H4A3, DSHB) antibodies targeting early endosomes and lysosomes, respectively. Subsequently, Alexa Fluor® 488-labeled secondary antibody goat anti-mouse (Thermo Fischer) was added at a concentration of 8 μg/ml and incubated for 1 h at room temperature. Cells were counterstained with 2.5 μg/ml Phalloidin-TRITC (Sigma-Aldrich) and 100 ng/ml DAPI for 1 h. Between each step, cells were washed three times with 0.05% PBS-Tween. Images were acquired using a Leica SP8X confocal microscope (Leica) and 63×/1.4 oil-immersion objective. Image processing and analysis was performed using Fiji (National Institutes of Health, Bethesda, USA) software version 1.50 [34].

2.9. ADAMTS5 silencing in TNF-α/OSM-stimulated OA chondrocytes in 3D culture

To evaluate the silencing efficiency of the gapmer, the *in vitro* model was cultured for 7 and 14 days. ASO 1, 3 or anti-ADAMTS5 siRNA were embedded in the top hydrogel at concentrations of 5 (7 and 14 days) and 10 μM (14 days). After polymerization, the hydrogels were incubated with DMEM supplemented with 5 μM ε-aminocaproic acid (Sigma-Aldrich) to delay fibrin degradation [35], 10 ng/ml recombinant human TNF-α and 1 ng/ml OSM. Medium was replaced twice a week and hydrogels were harvested for downstream analysis at days 7 and 14. The expression of *ADAMTS5* and the housekeeping genes glyceraldehyde 3-phosphate dehydrogenase (*GAPDH), ribosomal protein L19 (RPL19)* and succinate dehydrogenase complex subunit A (*SDHA)* were measured by qPCR. *CTNNBIP1* and *ADAMTS4* expression levels were analyzed as a control for off target effects. Cells embedded in top and bottom hydrogels were analyzed individually.

2.10. RNA isolation and real-time PCR (qPCR)

Total RNA was isolated in TRIzol Reagent (Invitrogen) according to the manufacturer's instructions. RNA was dissolved in DNAse/RNAse-Free water (Qiagen). Total RNA (200 ng–500 ng) was converted to cDNA by High Capacity cDNA Reverse Transcription Kit (Thermo Fischer Scientific) using an iCycler Thermal Cycler (Bio-Rad) according with the manufacturer's instructions. Real-time PCR reactions were performed using the iTAQ SYBR Green Reaction Mix Kit Mastermix (Bio-Rad) reaction kit according to the manufacturer's instructions in an iCycler CFX384 Touch thermal cycler (Bio-Rad). Reactions were prepared in 10 μl total volume with 0.92 μl PCR-H_2O, 0.04 μl forward primer (0.4 μM), 0.04 μl reverse primer (0.4 μM) and 5 μl iTAQ SYBR Green Reaction Mix (BioRad) to which 4 μl of fifty times diluted cDNA was added as template. Expression of *ADAMTS5, ADAMTS4*, *CTNNBIP1,* and the housekeeping genes *GAPDH, RPL19* and *SDHA* were analyzed by a three-step amplification qPCR. As mentioned above, *18S* was used as housekeeping gene for the screening experiments. Data analysis and Cq values were obtained with a Bio-Rad CFX Manager 3.1 (Bio-Rad). In order to generate relative gene expression, the Pfaffl method was used to account for differences in primer efficiencies [36]. Details of primers used in real-time PCR are listed in **Table S1**. The amplified PCR fragment extended over at least one exon border.

2.11. Statistical analysis

All data were analyzed using IBM® SPSS® Statistics version 21. Data were all normally distributed but violated the assumption of homogeneity of variances. One-way analysis of variance (One-way ANOVA) was used together with Welch test for the equality of the means. Post-hoc comparisons across groups were carried out using the Games-Howell post-hoc test. All the biological experiments were performed in three different donors ($n = 3$). For every condition 4 biological replicates were used.

3. Results

3.1. Selection of anti-ADAMTS5 ASO sequences in 2D chondrocyte culture

A set of 3 gapmers (ASOs 2, 3 and 4) targeting human *ADAMTS5* were designed and screened for *ADAMTS5* silencing. At 1000 nM, gene silencing was shown to be higher for all donors with ASO 3, with above 10-fold (> 90%) knockdown (Fig. 2a). In contrast, ASOs 2 and 4 did not mediate significant *ADAMTS5* silencing in comparison with non-treated cells. A non-targeting gapmer was used as a negative control (ASO 1) and did not significantly affect the expression of *ADAMTS5*. Based on this preliminary screening, ASO 3 was selected for subsequent experiments with ASO 1 used as a negative non-targeting control.

Gapmer-mediated silencing of TNF-α/OSM-stimulated *ADAMTS5* expression by OA chondrocytes was then investigated. Similar to siRNA, the gapmer sequence was shown to promote a 4-fold decrease in *ADAMTS5* at a concentration of 1000 nM. (Fig. 2b). Silencing was also observed at a concentration of 500 nM. The non-targeting gapmer ASO 1 did not alter *ADAMTS5* expression. Additionally, none of the concentrations were shown to be cytotoxic as measured by LDH release (**Fig. S1**).

3.2. Release kinetics

Gapmer incorporation efficiency, measured immediately after polymerization and washing, was shown to be around 93% for all conditions (Fig. 3a**, Table S1**). All formulations displayed similar release profiles, characterized by a burst release of 50% of the cargo within the first 24 h, followed by a gradual and sustained release until day 14. At day 14, 25–30% of the gapmer was still incorporated for all the tested formulations. The release during the first three days, gave rise to concentrations in the media of 100, 500, 200 and 1000 nM for the 150 μl/1 μM, 150 μl/5 μM, 300 μl/1 μM and 300 μl/5 μM hydrogel/gapmer formulations, respectively (Fig. 3b). Confocal imaging of the hydrogel/gapmer system at day 3 showed co-localization of the gapmer with the fibrin fibers, indicating possible interaction between the two molecules (Fig. 3c). This may explain the prolonged retention of the remaining 25–30% of gapmer inside the hydrogels. For subsequent 3D cell construct experiments, the formulations with 150 μl of hydrogel were used.

3.3. Gapmer diffusion and transfection of chondrocytes in 3D structures

To evaluate gapmer diffusion from the hydrogel and subsequent

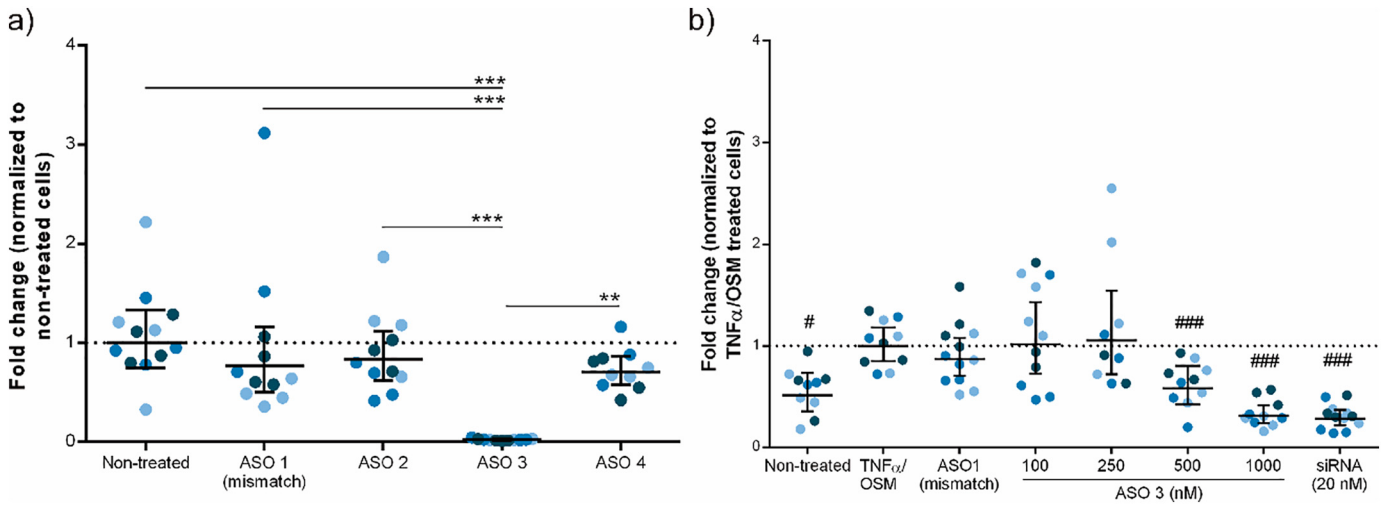


Fig. 2. ASO-mediated ADAMTS5 silencing in primary human OA chondrocytes. a) ASO sequence validation. *ADAMTS5* expression levels in primary human OA chondrocytes 72 h after treatment with 1000 nM of different ADAMTS5-targeting ASO sequences. b) Dose response to different concentrations of ASO 3. *ADAMTS5* expression levels in TNF-α/OSM-stimulated primary human OA chondrocytes 72 h after treatment with different concentrations of the "best-performing" sequence (ASO 3). ASO 1 (non-targeting) and anti-ADAMTS5 siRNA were used as negative and positive controls, respectively. Data are presented as geometric mean (mid-line) and 95% confidence interval (CI). Light Blue: Donor 1; Blue: Donor 2; Dark blue: Donor 3. * represents statistically significant differences as depicted; # represents statistically significant differences to the TNF-α/OSM group; (*$p < 0.05$, **$p < 0.01$ and ***$p < 0.001$). (For interpretation of the references to colour in this figure legend, the reader is referred to the web version of this article.)

entry into neighboring structures, a Cy5-gapmer-loaded hydrogel with chondrocytes was co-cultured for 3 days together with another hydrogel containing only chondrocytes. At day 3, the gapmer had diffused and penetrated into the adjacent hydrogel as shown by confocal microscopy (Fig. 4a). Co-localization was observed for DAPI and Cy5 signals, suggesting partial cellular accumulation of the released gapmer. Line-scan analysis further corroborated these findings. Histograms of the intensity profiles for DAPI and Cy5 confirmed the peak overlap for both signals (Fig. 4b).

For a more quantitative assay, a similar experimental set up was used at two different concentrations of Cy5 labeled gapmer (100 and 1000 nM). After 3 days of culture, hydrogels were digested and cells were processed for flow cytometry. As a control, hydrogels loaded with equal concentration of Cy5 labeled siRNA were taken along. The percentage of Cy5-positive cells was above 95% for all the ASO conditions and did not change significantly with gapmer concentration (**Fig. 4c** and **d**). A ten-fold increase in the mean fluorescence intensity is observed with the 1000 nM concentration compared with the 100 nM condition. Hydrogels containing siRNA showed similar patterns of fluorescence intensity and Cy5-positive cells.

3.4. Subcellular localization

As flow cytometry does not discriminate between association with the cell membrane or intracellular location, both hydrogels were digested, followed by plating of the cells in monolayer. Confocal imaging of the cells showed that the gapmer was located intracellularly and co-localized with lysosomes in cells from both top and bottom hydrogels (Fig. 5). No intracellular co-localization was found for siRNA, indicating the positivity observed in flow cytometric analysis was likely due to membrane association rather than internalization. The gapmer did not co-localize with early endosomes as shown by using a marker for early endosomes (EEA1) (**Fig. S2**). Gapmer accumulation in other vesicular structures other than lysosomes was suggested by punctate staining in structures negative for EEA1. Although intra-cellular trafficking may have been affected by the presence of PS modifications, co-localization using a PS ASO-Cy5 sequence was shown to be the same as the co-localization of the phosphodiester sequence (**Fig. S3**).

3.5. Gapmer-mediated silencing of ADAMTS5 in 3D cell constructs

Silencing of *ADAMTS5* in primary human OA chondrocytes upon TNF-α/OSM stimulation was assessed in the two-gel system. After day 7, ASO treatment induced a 2.5- (60%) and 3.3-fold (70%) decrease in *ADAMTS5* expression levels in the bottom and top hydrogels, respectively ($p < 0.001$, **Fig. 6a** and **b**).

At day 14, inhibition of *ADAMTS5* was also observed. A 35% reduction in *ADAMTS5* expression was observed in the bottom hydrogel (Fig. 6c), whereas a 45% silencing was observed for the top hydrogel ($p < 0.01$, Fig. 6d). Additionally, at a gapmer concentration of 10 μM, silencing appeared to increase to 50 and 55% in the bottom ($p < 0.05$) and top ($p < 0.001$) hydrogels, respectively. Both ASO 1 (non-targeting) and siRNA showed no knockdown of *ADAMTS5* expression at any of the studied timepoints. None of the tested sequences affected the levels of *ADAMTS4* gene expression (**Fig. S4**). However, a trend was noted towards a knockdown of *CTNNBIP1* by ASO 3 (Fig. 7) at day 7, which was lost at day 14. Regardless, gapmer effect on *ADAMTS5* expression was shown to be direct and not mediated through CTNNBIP1 activity, as was shown by siRNA-mediated silencing of the latter gene (**Fig. S5**).

4. Discussion

The ADAMTS enzyme family, in particular ADAMTS4 and ADAMTS5, play pivotal roles in proteoglycan degradation in OA, and inhibition of these molecules have proved to be beneficial for cartilage repair [11]. Antisense technologies offer unprecedented advantages when compared to other small molecule drugs, due to their higher target specificity and duration of action associated with arrest or interference with translation. Modified ASO gapmers are especially attractive due to their enhanced stability and capacity for unassisted internalization that offers gene silencing without the necessity for a transfection agent, which may simplify clinical translation.

In this study, we show proof-of-concept for the feasibility of hydrogel-based delivery of cells and gapmers for long-term silencing of OA-related genes. For this purpose, we established a culture model composed of two F:HA hydrogel constructs, one containing gapmers and OA chondrocytes mimicking a clinically implanted scaffold, and

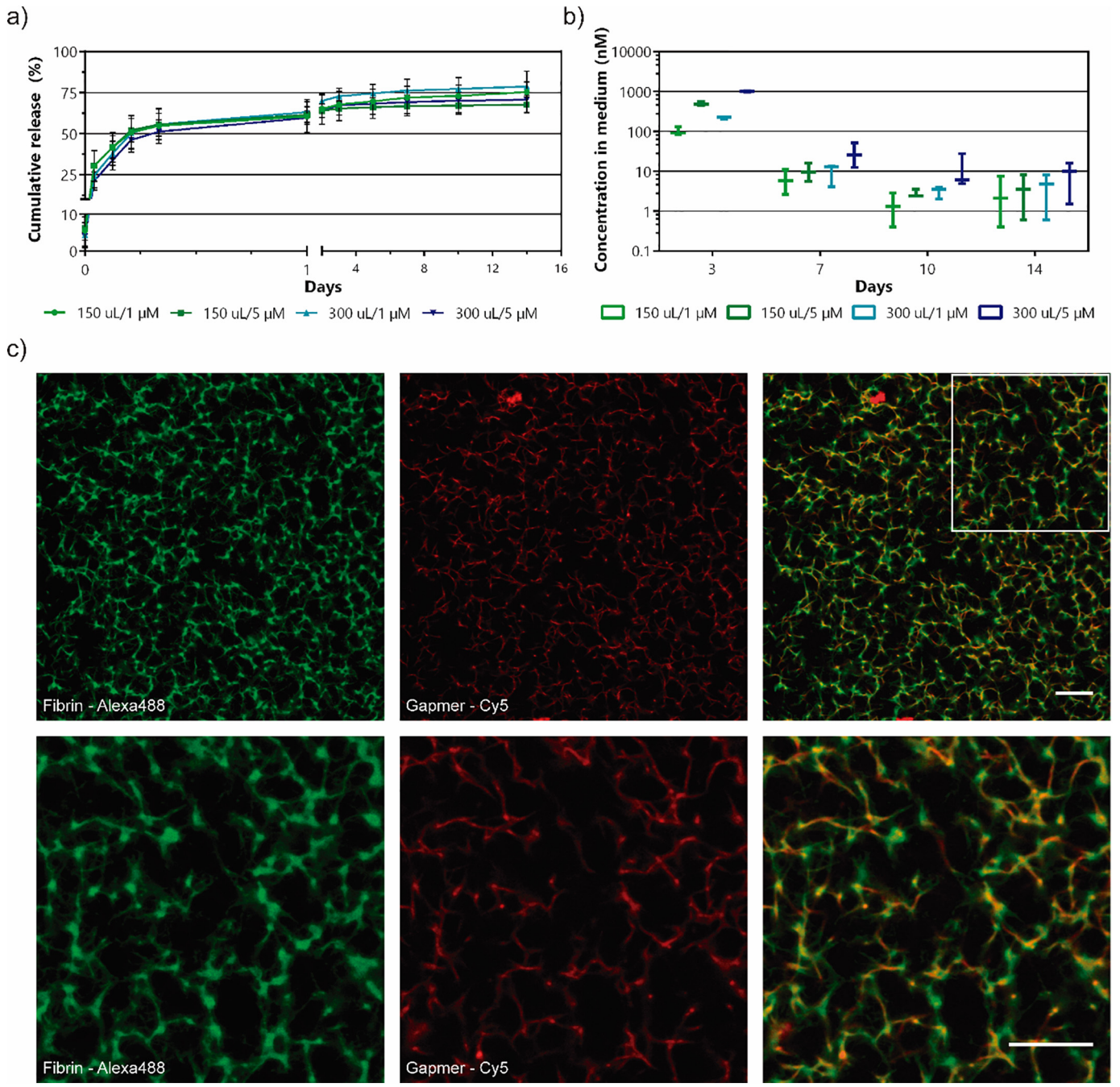
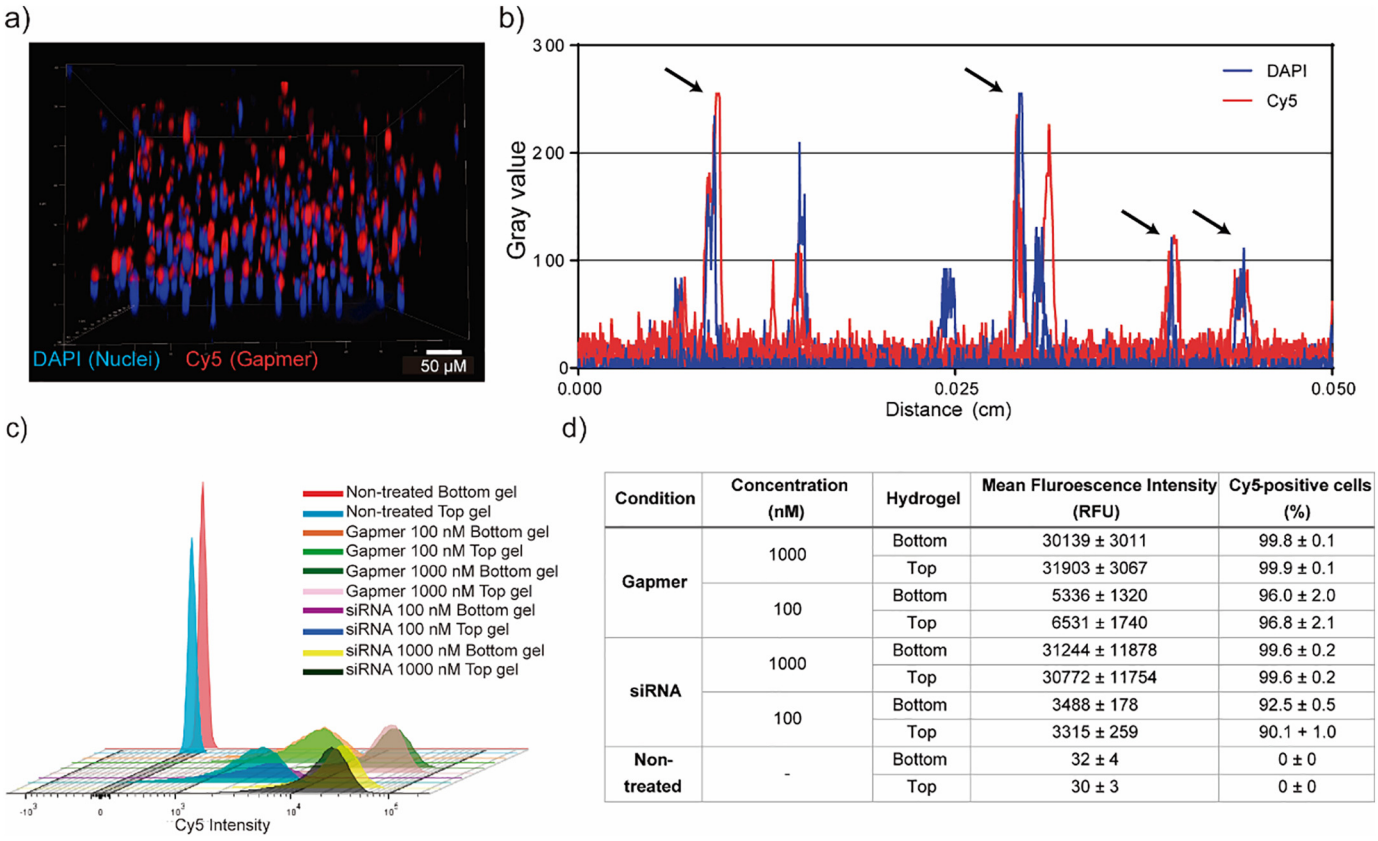


Fig. 3. Gapmer release profiles. a) Cumulative release profiles of different hydrogel/gapmer formulations. b) Gapmer concentration in the medium. Different concentrations of Cy5-labeled ASO (1 and 5 µM) were incorporated into different F:HA hydrogel volumes (150 and 300 µl). c) Co-localization of fibrin strands with gapmers. Fibrin was detected using an anti-fibrin antibody and an Alexa Fluor® 488-labeled secondary antibody. Green: Fibrin; Red: Cy5-gapmer. Hydrogels were imaged using a confocal microscope. Bottom row represents a zoomed in picture of top row (white square). Scale bar: 10 µm. (For interpretation of the references to colour in this figure legend, the reader is referred to the web version of this article.)

another one containing only OA chondrocytes mimicking resident joint cells. A sustained release for up to 14 days was found, with ≈ 25% of the gapmer retained at day 14, most likely associated with fibrin binding. Similar release profiles were observed across all the formulations, suggesting the system is not yet saturated, and higher gapmer concentrations can further be incorporated. Furthermore, efficient *ADAMTS5* knockdown in 3D constructs of OA chondrocytes was observed at days 7 and 14 for gapmer concentrations of 5 and 10 µM.

The two other ASO sequences, although sharing the same targeting moiety, display significant differences in silencing activities. The differences are likely due to varying lengths and LNA composition, since one is 17-nucleotide long and has four flanking LNAs in comparison with the other 15-nucleotide ASO 3 contained three flanking LNAs. Even though counterintuitive, it has previously been shown that shorter ASOs with lower affinity can potentially perform better than longer ASOs with higher affinity for the same targeting site [37–39]. This is attributed to diminished accessibility to the target region for the larger ASOs, or by an increased probability for the formation of secondary structures [40]. Clearly, there is a trade-off reduction of off-target effects by increasing gapmer length while maintaining its binding affinity to the target region (*i.e.* by lowering LNA content) might due to increased mismatched basepairs with the off-target region [40].



Condition	Concentration (nM)	Hydrogel	Mean Fluroescence Intensity (RFU)	Cy5-positive cells (%)
Gapmer	1000	Bottom	30139 ± 3011	99.8 ± 0.1
		Top	31903 ± 3067	99.9 ± 0.1
	100	Bottom	5336 ± 1320	96.0 ± 2.0
		Top	6531 ± 1740	96.8 ± 2.1
siRNA	1000	Bottom	31244 ± 11878	99.6 ± 0.2
		Top	30772 ± 11754	99.6 ± 0.2
	100	Bottom	3488 ± 178	92.5 ± 0.5
		Top	3315 ± 259	90.1 + 1.0
Non-treated	-	Bottom	32 ± 4	0 ± 0
		Top	30 ± 3	0 ± 0

Fig. 4. Gapmer diffusion and cellular association. a) 3D reconstruction of 350 µm of the bottom hydrogel 72 h after culture with Cy5-labeled gapmer in the top hydrogel. Blue: DAPI, Red: Cy5. b) Line-scan analysis of intensity profiles for DAPI and Cy5. c) Representative flow cytometric analysis of OA chondrocytes cultured in the bottom and top hydrogels in the presence of 100 and 1000 nM gapmer or siRNA. d) Mean Fluorescence intensity and percentage of Cy5-positive cells. (For interpretation of the references to colour in this figure legend, the reader is referred to the web version of this article.)

Additionally, the number and type of chemical modifications to the backbone of the ASOs were also shown to play a role in silencing efficiencies [37,39]. Altogether, these parameters are thought to affect the internalization capability of the ASOs, intracellular trafficking [39], coupling and uncoupling to target mRNA before and after RNAse H1 cleavage, as well as RNAse H1 recruitment [41]. Hence, these findings show ASO design and respective modifications are crucial steps for an efficient antisense activity [25].

Additional validation of the most active gapmer was performed in TNF-α/OSM-stimulated OA chondrocytes mimicking thereby the inflammatory joint environment. The selected sequence was shown to produce efficient silencing at concentrations above 500 nM and to yield *ADAMTS5* knockdown levels comparable to lipofectamine/siRNA control. The gapmer concentrations used in this study were efficient in the low micromolar range, as reported in other studies [22,25,26,42], in contrast to the 50-times lower concentrations required for siRNA. Yet the absence of transfection agents shows superiority of the gapmers over siRNAs, which corroborates previous studies on limited unassisted internalization of siRNAs [43].

From a clinical perspective it is important that sustained local release of the therapeutic molecule is achieved [19,30]. The F:HA hydrogel selected as a model system is currently being tested in clinical trials and fibrin and hyaluronic acid are already clinically used as cell carrier in surgical procedures [44,45], and in intra-articular injections for joint lubrication [46], respectively. The combination of ASOs with delivery platforms allows for sustained and prolonged silencing of their target genes, decreasing matrix degradation rate and enhancing repair and regeneration of the damaged tissue by both transplanted and endogenous cells.

Upon incorporation in the F:HA hydrogel, a 14-day long release was observed and, at the endpoint, 25% of the gapmer remained within the hydrogel. It is worth noting that release experiments were performed in the absence of cells. The presence of cells within the hydrogel may have led to faster release profiles, due to higher degradation and contraction of the construct. However, upon implantation of the hydrogel within an articular focal lesion, diffusion would be limited mainly to the area exposed to synovial fluid, therefore, decreasing the surface-to-volume ratio, and theoretically, promoting a slower release. Gapmer retention at day 14 is likely due to electrostatic and/or hydrophobic interactions with fibrin strands, as previously demonstrated [47]. Hence, these results suggest that by varying fibrin and hyaluronic acid content, release kinetics can be further tuned.

The mechanisms by which gapmers are internalized are not fully understood yet, however some studies have proposed a two-step mechanism initiated by adsorption to the cell membrane, and subsequent internalization through multiple endocytic pathways [26–29]. Here, LNA-based ASOs were shown to be able to penetrate into a secondary three-dimensional cell construct and transfect “resident” cells upon release from the delivery platform. High cellular association rates were observed for both ASO and siRNA sequences, yet confocal imaging confirmed that only ASOs were able to enter cells as seen by cytoplasmic localization and lysosomal co-localization. Gapmer accumulation upon “gymnotic” delivery was also observed in vesicular structures other than lysosomes, which may have represented the so-called P-bodies [25,28,29], perinuclear structures [28], or others as reported in previous studies.

To what extent the gapmers in the lysosomes and the unspecified cytoplasmic aggregates found were active is not completely clear. Additionally, RNAse H1 is known to be present and mediate ASO-induced mRNA cleavage in both in cytoplasm and nuclei [29,48].

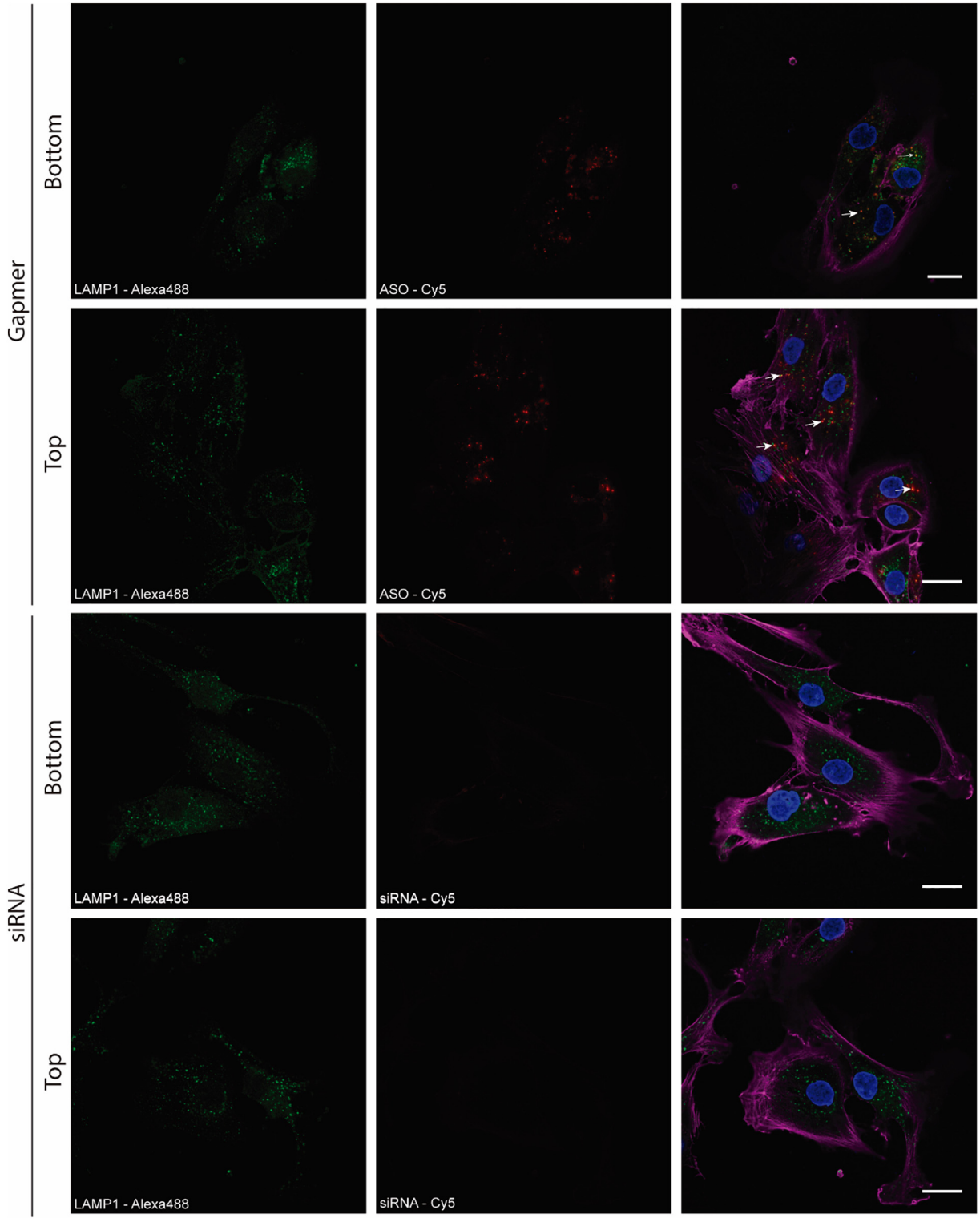


Fig. 5. Co-localization of ASOs and siRNA. OA chondrocytes were harvested from both bottom and top F:HA hydrogels after 3 days of culture and plated in monolayer for 24 h. Lysosomal staining was performed using an anti-LAMP1 primary antibody and an Alexa Fluor® 488-labeled secondary antibody. Cells were counterstained with DAPI and Phalloidin-TRITC. Green: LAMP1 (Lysosomes); Red: Cy5-gapmer/Cy5-siRNA; Blue: Nuclei; Purple: F-actin. White arrows indicate lysosomal co-localization. Scale bar: 20 μm. (For interpretation of the references to colour in this figure legend, the reader is referred to the web version of this article.)

Accordingly, the silencing and imaging results from the current study corroborate previous findings that nuclear localization is not required for effective ASO-mediated silencing [25,28,29]. Additionally, the possibility of diffuse cytoplasmic distribution cannot be discarded.

After 1 week, effective silencing was found in both hydrogel constructs, suggesting proof of principle of delivery to adjacent tissues *in vivo*. Yet, relatively lower silencing was found after a longer period of time. Most likely, hydrogel loading and hence silencing can be optimized further, as was suggested by the effects of the higher loading. At the current release profiles, the highest loading applied would

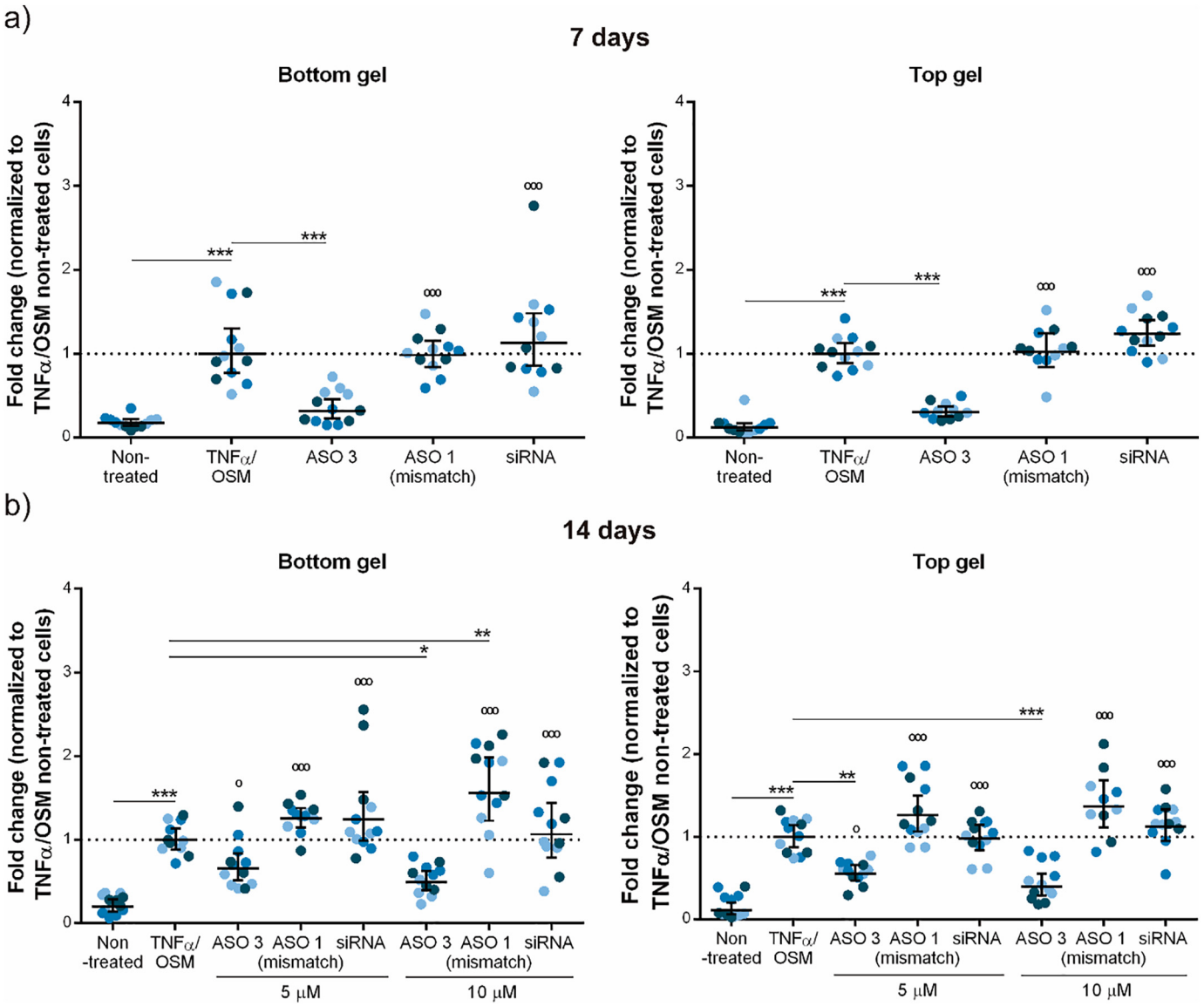


Fig. 6. Long-term gapmer-mediated ADAMTS5 knockdown in 3D cell constructs. Fold change in *ADAMTS5* gene expression in both top and bottom F:HA hydrogels after 7 (a) and 14 (b) days of culture. ASO and siRNA sequences were incorporated in the F:HA hydrogel together with human OA chondrocytes and co-cultured with a secondary F:HA hydrogel containing cells only. Data are presented as geometric mean (mid-line) and 95% confidence interval (CI). Experiment was performed in 3 biological replicates. Individual data points are represented in the graphs. Light Blue: Donor 1; Blue: Donor 2; Dark blue: Donor 3. * represents statistically significant differences to the TNF-α/OSM group; ° represents statistically significant differences to the non-treated group. (*$p < 0.05$, **$p < 0.01$ and ***$p < 0.001$). (For interpretation of the references to colour in this figure legend, the reader is referred to the web version of this article.)

correspond to a maximum concentration in the lower range of non-toxic concentrations previously reported [25,26,42]. In addition, TNF-α and OSM levels in synovial fluid of OA patients were shown to be within in the pg/ml range, hence at least 100-times lower than used in this study [49–51]. Therefore, the 5–6 fold increase of *ADAMTS5* expression observed in this study, which was shown to be only 2.4-fold in damaged cartilage area compared to healthy cartilage [52], may have been more difficult to silence.

Upon checking for off-target effects, *ADAMTS4* was not silenced by the gapmer sequence used, but *CTNNBIP1* expression did appear to be inhibited at day 7, although statistical significance was not reached. CTNNBIP1 is a protein that negatively regulates the β-catenin/Wnt pathway by preventing interaction between β-catenin and transcription factor 4 [53]. The ADAMTS5 silencing was not mediated by CTNNBIP1, as shown by the lack of effect on ADAMTS5 expression upon siRNA-mediated silencing of CTNNBIP1. To what extent the limited effects on *CTNNBIP1* found here will affect cartilage metabolism is unclear, as little is known about the role of this gene in this tissue. However, the notion that overexpression of this gene in mice caused disorders in cartilage development [54], may even suggest silencing may be beneficial.

Although the initially envisaged clinical application of the current system is cartilage resurfacing in OA joints, gapmer delivery can be extended towards other orthopedic applications. Acute and traumatic injuries to the knee such as meniscus tears, anterior cruciate ligament injury or cartilage defects are known to be major risk factors for the development of post-traumatic OA [55], which is most likely related to the increased production of several MMPs, aggrecanases and pro-inflammatory cytokines [56–59]. Indeed, ADAMTS4 activity was found to be a major predictor of postoperative outcome following (M)ACI for focal cartilage defect repair [60]. The use of the current hydrogel-gapmer construct may therefore also enhance the treatment outcome of joint traumas such as cartilage defects, either as add on to (M)ACI, or as cell free system in microfracture for smaller sized defects [61,62].

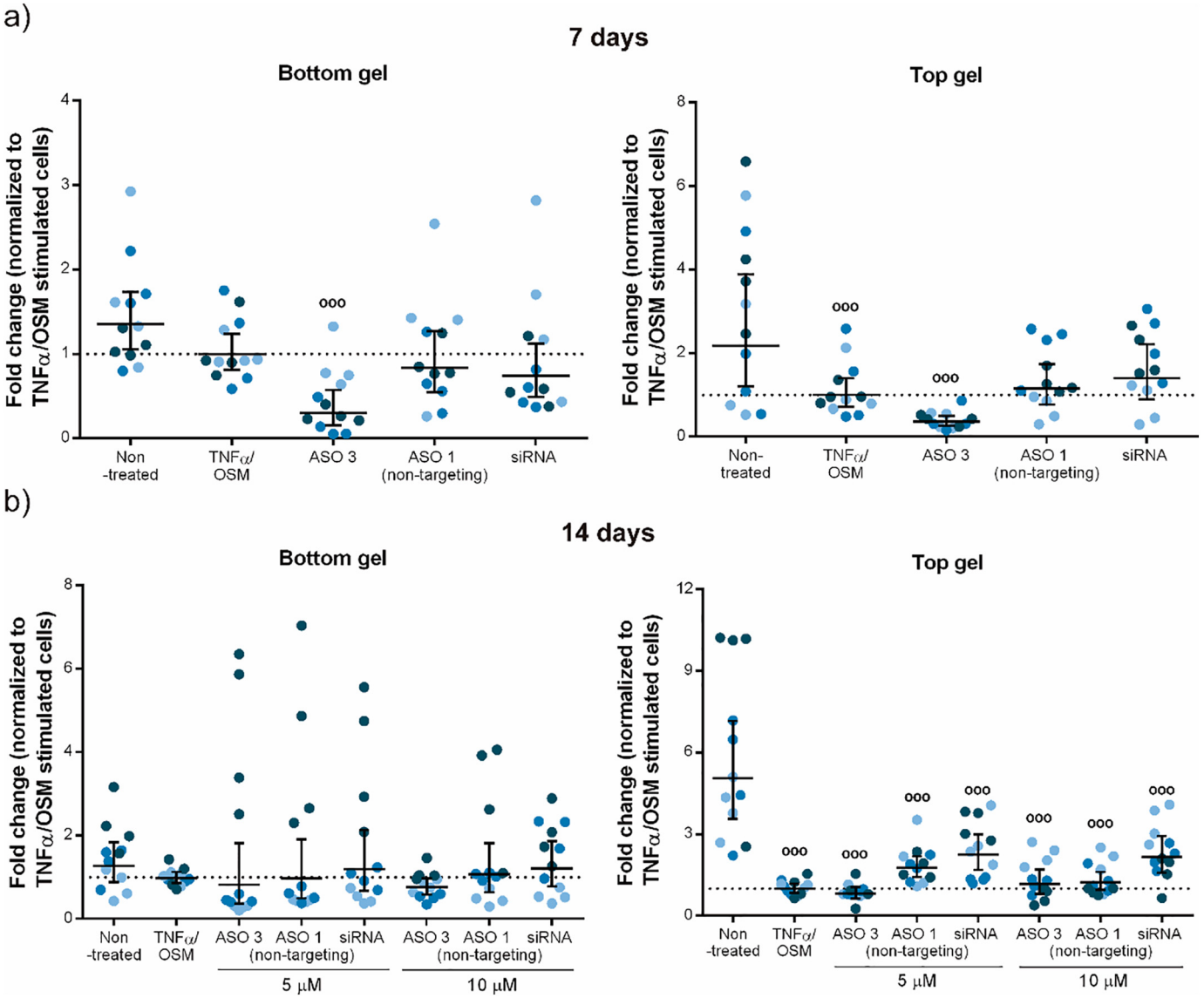


Fig. 7. *CTNNBIP1* expression. Fold change in *CTNNBIP1* expression in both top and bottom F:HA hydrogels after 7 (a) and 14 (b) days of culture. ASO and siRNA sequences were incorporated in the F:HA hydrogel together with human OA chondrocytes and co-cultured with a secondary F:HA hydrogel containing cells only. Data are presented as geometric mean (mid-line) and 95% confidence interval (CI). Experiment was performed in 3 biological replicates. Individual data points are represented in the graph. Light Blue: Donor 1; Blue: Donor 2; Dark blue: Donor 3. ° represents statistically significant differences to the non-treated cells; (° $p < 0.05$, °° $p < 0.01$ and °°° $p < 0.001$). (For interpretation of the references to colour in this figure legend, the reader is referred to the web version of this article.)

Similarly, novel cell-based approaches towards meniscus repair could be enhanced using the current approach [63]. Importantly, the use of gapmers allows for further tailoring of treatment by mere selection of the target to be silenced. For example, we previously showed the feasibility of an anti-COX2 gapmer-loaded chitosan/hyaluronic acid hydrogel as a strategy for targeted knockdown of the inflammatory enzyme COX2, in OA chondrocytes [42]. Given the fact that OA is a very heterogeneous and multi-factorial disease, one can hypothesize that ASOs can be tailored in a patient-specific manner to target the most relevant genes.

Although the sequence described here may also affect *CTNNBIP1*, from a technological point of view this does not underplay the general applicability of this approach. From a clinical point of view the sequence used may even be more effective for this reason, although from a regulatory perspective a sequence targeting *ADAMTS5* only may be preferable.

In this work, we successfully introduce the strategy of combined delivery of cells and LNA-modified ASOs in a hydrogel-based scaffold for long-term knockdown of OA-related genes. The long-term release and prolonged silencing renders the proposed system an attractive strategy for intra-articular delivery of both cells and ASOs. As the hydrogel has already been approved for the treatment of OA, it likely is an ideal candidate for use in combination with drug delivery.

5. Conclusion

In this study, we show proof-of-concept for the combined delivery of cells and ASOs in hydrogel-based scaffold as a potential therapeutic strategy for cartilage re-surfacing and silencing of OA-related genes. The F:HA hydrogel platform displayed a 14-days sustained release of the incorporated ASO, and allowed for ASO uptake by primary human OA chondrocytes after diffusion into the hydrogel. Moreover, efficient ADAMTS5 knockdown was found. Future studies will be focused on *ex vivo* evaluation of the potential of LNA-based ASOs as new therapeutic agents for modulation of OA-related genes.

Acknowledgements

This project has received funding from the European Union's Horizon 2020 research and innovation programme under Marie Sklodowska-Curie grant agreement No. 642414 and the Dutch Arthritis Foundation (LLP12). The authors would like to thank Luís Garcia for providing the illustrations for the graphical abstract and Fig. 1.

Appendix A. Supplementary data

Supplementary data to this article can be found online at https://doi.org/10.1016/j.jconrel.2018.12.030.

References

[1] M.B. Goldring, S.R. Goldring, Osteoarthritis, J. Cell. Physiol. 213 (2007) 626–634, https://doi.org/10.1002/jcp.21258.
[2] H. Madry, F.P. Luyten, A. Facchini, Biological aspects of early osteoarthritis, Knee Surg. Sports Traumatol. Arthrosc. 20 (2011) 407–422, https://doi.org/10.1007/s00167-011-1705-8.
[3] M.B. Goldring, The role of the chondrocyte in osteoarthritis, Arthritis Rheum. 43 (2000) 1916–1926, https://doi.org/10.1002/1529-0131(200009)43:9<1916::AID-ANR2>3.0.CO;2-I.
[4] A.D. Woolf, B. Pfleger, Burden of major musculoskeletal conditions, Bull. World Health Organ. 81 (2003) 646–656.
[5] M.B. Goldring, F. Berenbaum, Emerging targets in osteoarthritis therapy, Curr. Opin. Pharmacol. 22 (2015) 51–63, https://doi.org/10.1016/j.coph.2015.03.004.
[6] M.L. Davies-Tuck, A.E. Wluka, Y. Wang, A.J. Teichtahl, G. Jones, C. Ding, F.M. Cicuttini, The natural history of cartilage defects in people with knee osteoarthritis, Osteoarthr. Cartil. 16 (2008) 337–342, https://doi.org/10.1016/j.joca.2007.07.005.
[7] E.B. Dam, J. Runhaar, S. Bierma-Zienstra, M. Karsdal, Cartilage cavity-an MRI marker of cartilage lesions in knee OA with Data from CCBR, OAI, and PROOF, Magn. Reson. Med. (2018), https://doi.org/10.1002/mrm.27130.
[8] C. Ding, F. Cicuttini, G. Jones, Tibial subchondral bone size and knee cartilage defects: relevance to knee osteoarthritis, Osteoarthr. Cartil. 15 (2007) 479–486, https://doi.org/10.1016/j.joca.2007.01.003.
[9] K. Hjelle, E. Solheim, T. Strand, R. Muri, M. Brittberg, Articular cartilage defects in 1,000 knee arthroscopies, Arthroscopy 18 (2002) 730–734, https://doi.org/10.1053/jars.2002.32839.
[10] R.A. Magnussen, W.R. Dunn, J.L. Carey, K.P. Spindler, Treatment of focal articular cartilage defects in the knee: a systematic review, Clin. Orthop. Relat. Res. 466 (2008) 952–962, https://doi.org/10.1007/s11999-007-0097-z.
[11] P. Verma, K. Dalal, ADAMTS-4 and ADAMTS-5: key enzymes in osteoarthritis, J. Cell. Biochem. 112 (2011) 3507–3514, https://doi.org/10.1002/jcb.23298.
[12] R.H. Song, M. D. Tortorella, A.M. Malfait, J.T. Alston, Z. Yang, E.C. Arner, D.W. Griggs, Aggrecan degradation in human articular cartilage explants is mediated by both ADAMTS-4 and ADAMTS-5, Arthritis Rheum. 56 (2007) 575–585, https://doi.org/10.1002/art.22334.
[13] J. Bondeson, S.D. Wainwright, S. Lauder, N. Amos, C.E. Hughes, The role of synovial macrophages and macrophage-produced cytokines in driving aggrecanases, matrix metalloproteinases, and other destructive and inflammatory responses in osteoarthritis, Arthritis Res Ther. 8 (2006) R187, , https://doi.org/10.1186/ar2099.
[14] H. Deng, H. O'Keefe, C.P. Davie, K.E. Lind, R.A. Acharya, G.J. Franklin, J. Larkin, R. Matico, M. Neeb, M.M. Thompson, T. Lohr, J.W. Gross, P.A. Centrella, G.K. O'Donovan, K.L. Bedard, K. van Vloten, S. Mataruse, S.R. Skinner, S.L. Belyanskaya, T.Y. Carpenter, T.W. Shearer, M.A. Clark, J.W. Cuozzo, C.C. Arico-Muendel, B.A. Morgan, Discovery of highly potent and selective small molecule ADAMTS-5 inhibitors that inhibit human cartilage degradation via encoded library technology (ELT), J. Med. Chem. 55 (2012) 7061–7079, https://doi.org/10.1021/jm300449x.
[15] Y. He, Q. Zheng, M. Jiang, S. Sun, T.G. Christiansen, M. Kassem, M.A. Karsdal, A.C. Bay-Jensen, The effect of protease inhibitors on the induction of osteoarthritis-related biomarkers in bovine full-depth cartilage explants, PLoS One 10 (2015) e0122700, , https://doi.org/10.1371/journal.pone.0122700.
[16] P. Chen, S. Zhu, Y. Wang, Q. Mu, Y. Wu, Q. Xia, X. Zhang, H. Sun, J. Tao, H. Hu, P. Lu, H. Ouyang, The amelioration of cartilage degeneration by ADAMTS-5 inhibitor delivered in a hyaluronic acid hydrogel, Biomaterials 35 (2014) 2827–2836, https://doi.org/10.1016/j.biomaterials.2013.12.076.
[17] S.S. Glasson, R. Askew, B. Sheppard, B. Carito, T. Blanchet, H.L. Ma, C.R. Flannery, D. Peluso, K. Kanki, Z. Yang, M.K. Majumdar, E.A. Morris, Deletion of active ADAMTS5 prevents cartilage degradation in a murine model of osteoarthritis, Nature 434 (2005) 644–648, https://doi.org/10.1038/nature03369.
[18] J. Larkin, T.A. Lohr, L. Elefante, J. Shearin, R. Matico, J.L. Su, Y. Xue, F. Liu, C. Genell, R.E. Miller, P.B. Tran, A.M. Malfait, C.C. Maier, C.J. Matheny, Translational development of an ADAMTS-5 antibody for osteoarthritis disease modification, Osteoarthr. Cartil. 23 (2015) 1254–1266, https://doi.org/10.1016/j.joca.2015.02.778.
[19] N. Gerwin, C. Hops, A. Lucke, Intraarticular drug delivery in osteoarthritis, Adv. Drug Deliv. Rev. 58 (2006) 226–242, https://doi.org/10.1016/j.addr.2006.01.018.
[20] S.F. Dowdy, Overcoming cellular barriers for RNA therapeutics, Nat. Biotechnol. 35 (2017) 222–229, https://doi.org/10.1038/nbt.3802.
[21] K.A. Howard, Delivery of RNA interference therapeutics using polycation-based nanoparticles, Adv. Drug Deliv. Rev. 61 (2009) 710–720, https://doi.org/10.1016/j.addr.2009.04.001.
[22] C. Wahlestedt, P. Salmi, L. Good, J. Kela, T. Johnsson, T. Hokfelt, C. Broberger, F. Porreca, J. Lai, K. Ren, M. Ossipov, A. Koshkin, N. Jakobsen, J. Skouv, H. Oerum, M.H. Jacobsen, J. Wengel, Potent and nontoxic antisense oligonucleotides containing locked nucleic acids, Proc. Natl. Acad. Sci. U. S. A. 97 (2000) 5633–5638, https://doi.org/10.1073/pnas.97.10.5633.
[23] N. Dias, C.A. Stein, Antisense oligonucleotides: basic concepts and mechanisms, Mol. Cancer Ther. 1 (2002) 347–355.
[24] P.H. Hagedorn, R. Persson, E.D. Funder, N. Albaek, S.L. Diemer, D.J. Hansen, M.R. Moller, N. Papargyri, H. Christiansen, B.R. Hansen, H.F. Hansen, M.A. Jensen, T. Koch, Locked nucleic acid: modality, diversity, and drug discovery, Drug Discov. Today 23 (2018) 101–114, https://doi.org/10.1016/j.drudis.2017.09.018.
[25] C.A. Stein, J.B. Hansen, J. Lai, S. Wu, A. Voskresenskiy, A. Hog, J. Worm, M. Hedtjarn, N. Souleimanian, P. Miller, H.S. Soifer, D. Castanotto, L. Benimetskaya, H. Orum, T. Koch, Efficient gene silencing by delivery of locked nucleic acid antisense oligonucleotides, unassisted by transfection reagents, Nucleic Acids Res. 38 (2010) e3, https://doi.org/10.1093/nar/gkp841.
[26] H.S. Soifer, T. Koch, J. Lai, B. Hansen, A. Hoeg, H. Oerum, C.A. Stein, Silencing of gene expression by gymnotic delivery of antisense oligonucleotides, Methods Mol. Biol. 815 (2012) 333–346, https://doi.org/10.1007/978-1-61779-424-7_25.
[27] R.L. Juliano, X. Ming, K. Carver, B. Laing, Cellular uptake and intracellular trafficking of oligonucleotides: implications for oligonucleotide pharmacology, Nucleic Acid Ther. 24 (2014) 101–113, https://doi.org/10.1089/nat.2013.0463.
[28] D. Castanotto, M. Lin, C. Kowolik, L. Wang, X.Q. Ren, H.S. Soifer, T. Koch, B.R. Hansen, H. Oerum, B. Armstrong, Z. Wang, P. Bauer, J. Rossi, C.A. Stein, A cytoplasmic pathway for gapmer antisense oligonucleotide-mediated gene silencing in mammalian cells, Nucleic Acids Res. 43 (2015) 9350–9361, https://doi.org/10.1093/nar/gkv964.
[29] S.T. Crooke, S. Wang, T.A. Vickers, W. Shen, X.H. Liang, Cellular uptake and trafficking of antisense oligonucleotides, Nat. Biotechnol. 35 (2017) 230–237, https://doi.org/10.1038/nbt.3779.
[30] A.G. Bajpayee, A.J. Grodzinsky, Cartilage-targeting drug delivery: can electrostatic interactions help? Nat. Rev. Rheumatol. 13 (2017) 183–193, https://doi.org/10.1038/nrrheum.2016.210.
[31] L. Sepp-Lorenzino, M.K. Ruddy, Challenges and Opportunities for local and Systemic delivery of siRNA and Antisense Oligonucleotides, Clin. Pharmacol. Ther. 84 (2008) 628–632.
[32] X. Zhao, F. Pan, C.M. Holt, A.L. Lewis, J.R. Lu, Controlled delivery of antisense oligonucleotides: a brief review of current strategies, Expert Opin. Drug Deliv. 6 (2009) 673–686, https://doi.org/10.1517/17425240902992894.
[33] M.J. Domingues, F. Rambow, B. Job, L. Papon, W.G. Liu, L. Larue, J. Bonaventure, I.C.A.T. Beta-Catenin Inhibitor, Modulates the invasive motility of melanoma cells, Cancer Res. 74 (2014) 1983–1995, https://doi.org/10.1158/0008-5472.Can-13-0920.
[34] J. Schindelin, I. Arganda-Carreras, E. Frise, V. Kaynig, M. Longair, T. Pietzsch, S. Preibisch, C. Rueden, S. Saalfeld, B. Schmid, J.Y. Tinevez, D.J. White, V. Hartenstein, K. Eliceiri, P. Tomancak, A. Cardona, Fiji: an open-source platform for biological-image analysis, Nat. Methods 9 (2012) 676–682, https://doi.org/10.1038/nmeth.2019.
[35] L. Kupcsik, M. Alini, M.J. Stoddart, Epsilon-aminocaproic acid is a useful fibrin degradation inhibitor for cartilage tissue engineering, Tissue Eng. A 15 (2009) 2309–2313, https://doi.org/10.1089/ten.tea.2008.0400.
[36] M.W. Pfaffl, A new mathematical model for relative quantification in real-time RT-PCR, Nucleic Acids Res. 29 (2001) e45.
[37] M. Frieden, S.M. Christensen, N.D. Mikkelsen, C. Rosenbohm, C.A. Thrue, M. Westergaard, H.F. Hansen, H. Orum, T. Koch, Expanding the design horizon of antisense oligonucleotides with alpha-L-LNA, Nucleic Acids Res. 31 (2003) 6365–6372, https://doi.org/10.1093/nar/gkg820.
[38] E.M. Straarup, N. Fisker, M. Hedtjarn, M.W. Lindholm, C. Rosenbohm, V. Aarup, H.F. Hansen, H. Orum, J.B.R. Hansen, T. Koch, Short locked nucleic acid antisense oligonucleotides potently reduce apolipoprotein B mRNA and serum cholesterol in mice and non-human primates, Nucleic Acids Res. 38 (2010) 7100–7111, https://doi.org/10.1093/nar/gkq457.
[39] R. Stanton, S. Sciabola, C. Salatto, Y. Weng, D. Moshinsky, J. Little, E. Walters, J. Kreeger, D. Dimattia, T. Chen, T. Clark, M. Liu, J. Qian, M. Roy, R. Dullea, Chemical modification study of antisense gapmers, Nucleic Acid. Ther. 22 (2012) 344–359, https://doi.org/10.1089/nat.2012.0366.
[40] P.H. Hagedorn, M. Pontoppidan, T.S. Bisgaard, M. Berrera, A. Dieckmann, M. Ebeling, M.R. Moller, H. Hudlebusch, M.L. Jensen, H.F. Hansen, T. Koch, M. Lindow, Identifying and avoiding off-target effects of RNase H-dependent antisense oligonucleotides in mice, Nucleic Acids Res. 46 (2018) 5366–5380, https://doi.org/10.1093/nar/gky397.
[41] L. Pedersen, P.H. Hagedorn, M.W. Lindholm, M. Lindow, A Kinetic model explains why shorter and less Affine Enzyme-recruiting Oligonucleotides can be more potent, Mol. Ther-Nucl. Acids. 3 (2014), https://doi.org/10.1038/mtna.2013.72.
[42] Y. Cai, E. Lopez-Ruiz, J. Wengel, L.B. Creemers, K.A. Howard, A hyaluronic acid-based hydrogel enabling CD44-mediated chondrocyte binding and gapmer oligonucleotide release for modulation of gene expression in osteoarthritis, J. Control. Release 253 (2017) 153–159, https://doi.org/10.1016/j.jconrel.2017.03.004.
[43] A. Muratovska, M.R. Eccles, Conjugate for efficient delivery of short interfering RNA (siRNA) into mammalian cells, FEBS Lett. 558 (2004) 63–68, https://doi.org/10.1016/S0014-5793(03)01505-9.
[44] F. Cortese, M. McNicholas, G. Janes, S. Gillogly, S.P. Abelow, A. Gigante, N. Coletti,

Arthroscopic delivery of matrix-induced autologous chondrocyte implant: International experience and technique recommendations, Cartilage. 3 (2012) 156–164, https://doi.org/10.1177/1947603511435271.
[45] T.S. de Windt, L.A. Vonk, I.C.M. Slaper-Cortenbach, R. Nizak, M.H.P. van Rijen, D.B.F. Saris, Allogeneic MSCs and recycled autologous chondrons mixed in a one-stage cartilage cell transplantion: a first-in-man trial in 35 patients, Stem Cells 35 (2017) 1984–1993, https://doi.org/10.1002/stem.2657.
[46] R.R. Bannuru, N.S. Natov, I.E. Obadan, L.L. Price, C.H. Schmid, T.E. McAlindon, Therapeutic trajectory of hyaluronic acid versus corticosteroids in the treatment of knee osteoarthritis: a systematic review and meta-analysis, Arthritis Care Res. 61 (2009) 1704–1711, https://doi.org/10.1002/art.24925.
[47] P.M.D. Moreno, A.R. Ferreira, D. Salvador, M.T. Rodrigues, M. Torrado, E.D. Carvalho, U. Tedebark, M.M. Sousa, I.F. Amaral, J. Wengel, A.P. Pêgo, Hydrogel-assisted antisense LNA Gapmer delivery for in situ gene silencing in spinal cord injury, Mol Ther-Nucl. Acids. 11 (2018) 393–406, https://doi.org/10.1016/j.omtn.2018.03.009.
[48] H.J. Wu, W.F. Lima, H. Zhang, A. Fan, H. Sun, S.T. Crooke, Determination of the role of the human RNase H1 in the pharmacology of DNA-like antisense drugs, J. Biol. Chem. 279 (2004) 17181–17189, https://doi.org/10.1074/jbc.M311683200.
[49] D.H. Manicourt, P. Poilvache, A. Van Egeren, J.P. Devogelaer, M.E. Lenz, E.J. Thonar, Synovial fluid levels of tumor necrosis factor alpha and oncostatin M correlate with levels of markers of the degradation of crosslinked collagen and cartilage aggrecan in rheumatoid arthritis but not in osteoarthritis, Arthritis Rheum-Us. 43 (2000) 281–288, https://doi.org/10.1002/1529-0131(200002)43:2<281::AID-ANR7>3.0.CO;2-7.
[50] K. Ozler, E. Aktas, C. Atay, B. Yilmaz, M. Arikan, S. Gungor, Serum and knee synovial fluid matrixmetalloproteinase-13 and tumor necrosis factor-alpha levels in patients with late stage osteoarthritis, Acta Orthop. Traumatol. Turc. 50 (2016) 670–673, https://doi.org/10.1016/j.aott.2015.11.003.
[51] H.K. Vincent, S.S. Percival, B.P. Conrad, A.N. Seay, C. Montero, K.R. Vincent, Hyaluronic Acid (HA) Viscosupplementation on Synovial Fluid Inflammation in knee Osteoarthritis: a pilot Study, Open Orthop J. 7 (2013) 378–384, https://doi.org/10.2174/1874325001307010378.
[52] S.L. Dunn, J. Soul, S. Anand, J.M. Schwartz, R.P. Boot-Handford, T.E. Hardingham, Gene expression changes in damaged osteoarthritic cartilage identify a signature of non-chondrogenic and mechanical responses, Osteoarthr. Cartil. 24 (2016) 1431–1440, https://doi.org/10.1016/j.joca.2016.03.007.
[53] Z. Wu, S. Zheng, Z. Li, J. Tan, Q. Yu, E2F1 suppresses Wnt/beta-catenin activity through transactivation of beta-catenin interacting protein ICAT, Oncogene 30 (2011) 3979–3984, https://doi.org/10.1038/onc.2011.129.
[54] M. Zhu, M. Chen, M. Zuscik, Q. Wu, Y.J. Wang, R.N. Rosier, R. J, D. Chen O'Keefe, Inhibition of beta-catenin signaling in articular chondrocytes results in articular cartilage destruction, Arthritis Rheum. 58 (2008) 2053–2064, https://doi.org/10.1002/art.23614.
[55] J. Lieberthal, N. Sambamurthy, C.R. Scanzello, Inflammation in joint injury and post-traumatic osteoarthritis, Osteoarthr. Cartil. 23 (2015) 1825–1834, https://doi.org/10.1016/j.joca.2015.08.015.
[56] A. Kwapisz, M. Chojnacki, M. Domzalski, A. Grzegorzewski, M. Synder, Do gene expression changes in articular cartilage proteases of the synovial membrane correlate with expression changes of the same genes in systemic blood cells? Int. Orthop. 38 (2014) 649–654, https://doi.org/10.1007/s00264-013-2195-8.
[57] M. Bigoni, P. Sacerdote, M. Turati, S. Franchi, M. Gandolla, D. Gaddi, S. Moretti, D. Munegato, C.A. Augusti, E. Bresciani, R.J. Omeljaniuk, V. Locatelli, A. Torsello, Acute and late changes in intraarticular cytokine levels following anterior cruciate ligament injury, J. Orthop. Res. 31 (2013) 315–321, https://doi.org/10.1002/jor.22208.
[58] F.E. Watt, E. Paterson, A. Freidin, M. Kenny, A. Judge, J. Saklatvala, A. Williams, T.L. Vincent, Acute Molecular changes in Synovial Fluid following Human knee Injury: Association with early Clinical Outcomes, Arthritis Rheumatol. 68 (2016) 2129–2140, https://doi.org/10.1002/art.39677.
[59] R.H. Brophy, L.J. Sandell, M.F. Rai, Traumatic and degenerative meniscus tears have different gene expression signatures, Am. J. Sport Med. 45 (2017) 114–120, https://doi.org/10.1177/0363546516664889.
[60] K.T. Wright, J.H. Kuiper, J.B. Richardson, P. Gallacher, S. Roberts, The absence of detectable ADAMTS-4 (Aggrecanase-1) activity in synovial fluid is a predictive indicator of autologous chondrocyte implantation success, Am. J. Sport. Med. 45 (2017) 1806–1814, https://doi.org/10.1177/0363546517694027.
[61] J.R. Perera, P.D. Gikas, G. Bentley, The present state of treatments for articular cartilage defects in the knee, Ann. R. Coll. Surg. Engl. 94 (2012) 381–387, https://doi.org/10.1308/003588412X13171221592573.
[62] B.M. Devitt, S.W. Bell, K.E. Webster, J.A. Feller, T.S. Whitehead, Surgical treatments of cartilage defects of the knee: Systematic review of randomised controlled trials, Knee 24 (2017) 508–517, https://doi.org/10.1016/j.knee.2016.12.002.
[63] J.V. Korpershoek, T.S. de Windt, M.H. Hagmeijer, L.A. Vonk, D.B. Saris, Cell-based meniscus repair and regeneration: at the brink of clinical translation?: A systematic review of preclinical studies, Orthop. J. Sports Med. 5 (2017), https://doi.org/10.1177/2325967117690131.